13th World Conference on Earthquake Engineering
Vancouver, B.C., Canada
August 1-6, 2004
Paper No. 2474

STRUCTURAL PERFORMANCE OF EXTERIOR BEAM COLUMN JOINTS WITH MECHANICAL ANCHORAGE AT MAIN BARS

Juan Jose CASTRO[1], Hiroshi IMAI[2]

SUMMARY

In this research, the influence of the concrete strength, the lateral reinforcement ratio of the beam column joint and the anchor length of main bars with mechanical anchorages on the seismic behavior of exterior beam column joints was experimentally investigated.

Eleven beam column joints specimens were tested with the main bars of beams provided with mechanical anchorage devices. The variables for this study were the concrete strength (21, 36, 50, 70 N/mm^2), tensile strength of main bars (490, 690 N/mm^2) and failure type (beam bending failure types, joint shear failure type and anchorage failure type).

The specimens reinforced with high strength bars for beams showed enough anchor strength and ductility. For beam main bars a development length of 12 times the bar diameter and 3/4 of the column depth is needed to ensure the anchor strength.

INTRODUCTION

The number of high rise buildings (more than 60m in height) especially for residential buildings have increased significantly in the recent years in Japan. In this sense, the development of high strength materials and high strength steel bars presents a substantial increase. In this kind of structures not only high strength but also large size of bars are used for beams and columns. Thus the beam column joints bar arrangements become very complicated especially in case of exterior beam column joints where the beam bars must be anchored inside of the joint panel.

The anchor details, basically used for the exterior beam column joints are shown in Fig. 1. For the lower story buildings the beam main bars are usually anchored using the L type or U type anchorage as shown in Figs 1 (a) and (b). However for high-rise buildings where large size bars are used the joints become highly congested, and hence it arouses problems like increase of the labor costs and quality of the final structure since the concrete could be poorly placed inside the joint.

[1] Senior Researcher, Kabuki Construction Co. Ltd., Tokyo, Japan. Email:castro.j@kabuki.co.jp
[2] Professor, University of Tsukuba, Ibaraki, Japan., Email:imai@kz.tsukuba.ac.jp

To solve the problems expressed above, mechanical anchored were developed as shown in Fig. 1(c). In this case the forces that applied to the beam bars are to be resisted by bearing and bond forces inside the joints by the anchor plates and main bars, respectively. This type of devices contributes not only to the simplicity of the bar arrangements at the site but also to improve the quality control and the concrete cast can be easily executed.

There are several studies carried out on exterior beam column joints using mechanical anchorages [1], [2], [3], with concrete strength ranging between 24 and 60N/mm^2 and bar diameters between 16 and 19 mm. However, as expressed above the rise of the material strength and the use of large size diameters bars aroused uncertainties on the structural performance that needs to be clarified.

The present research focused on the structural performance of beam column joints when the beam bars are large size diameters like D25 and D32 provided with anchor plates. Also the influence of concrete strength, amount of lateral reinforcement inside the joint, and the anchor length on the seismic behavior was investigated. Special emphasis was placed on the bearing stresses of the anchor plates.

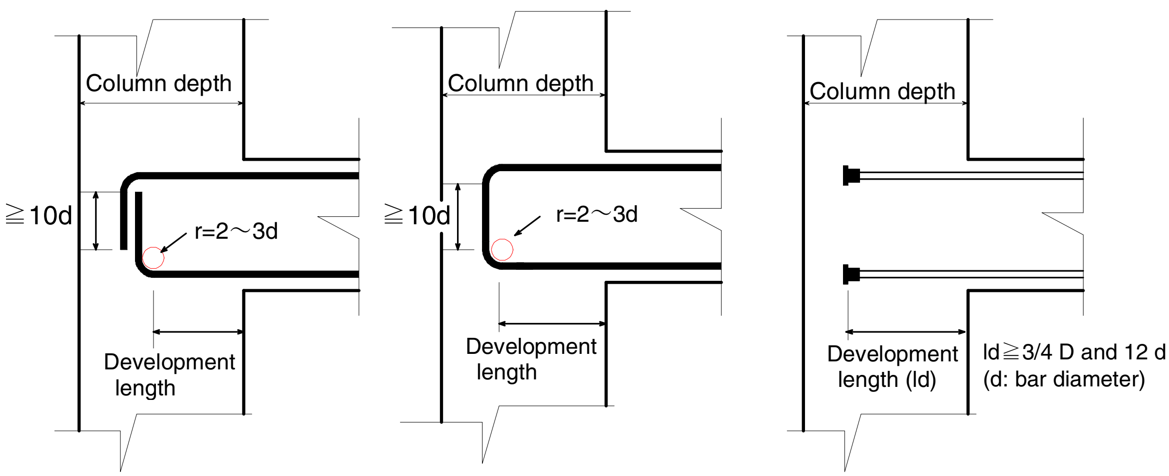

Fig. 1 Different types of anchorages

EXPERIMENTAL PROGRAM

Specimens

The specimens are listed in Table 1 and the typical specimen is shown in Fig. 2. The section of column is 400 mm x 400 mm, and the beam is 350 mm x 450 mm for all specimens, except for No.11 where the column is 600 mm x 600 mm and the beam is 530 mm x 600 mm. The sections of beams and columns are shown in Figs. 2 and 3.

The experiment was divided into two series, *Series A (SD490)* and *Series B (SD685)*. The *Series A* consists of 5 specimens (No.1 to No.5), with three of them designed as beam yielding failure type, and the other two to have shear failure at the beam column joint. In this series, the beam main bars were grade SD490 (specified yield strength is 490 N/mm^2). The *Series B* consists of 6 specimens (No.7 to No.12), with two of them designed to have beam flexural failure type and the other four to fail in shear at the beam column joint. In this series for the beam main bars, SD685 (specified yield strength is 685 N/mm^2) grade bars were used.

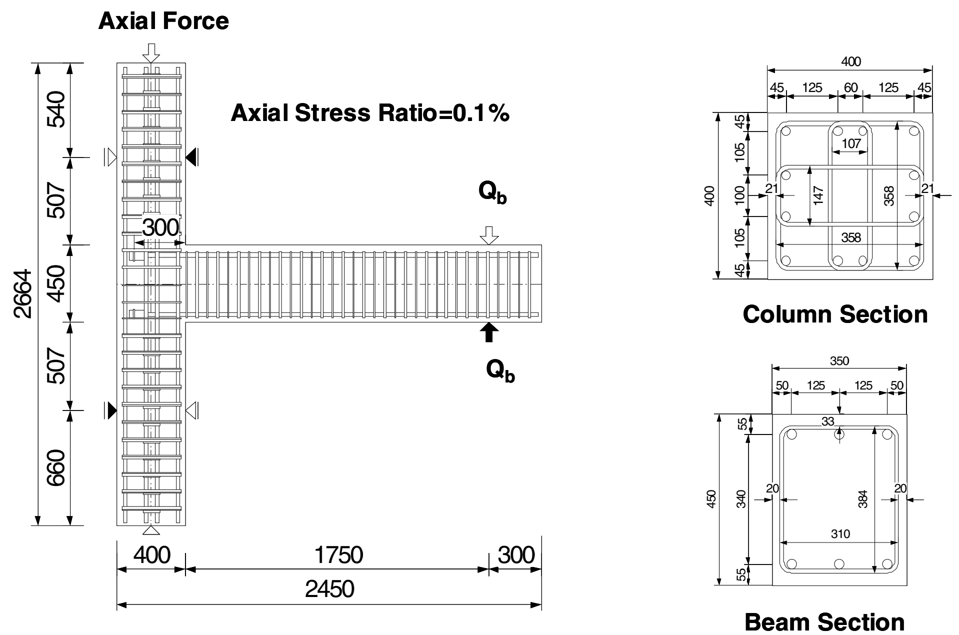

Fig. 2 Outline of specimens

Table 1 Outline of Specimens

Series	Spec.	Fc	Failure Mode	Section (mm) Col	Section (mm) Beam	Bars Beam	Bars Col.	Joint Reinf.	Anchor Length (mm)	Cover (mm) Rear	Cover (mm) Side
A	No.1	50	B	400 x 400	350 x 400	D25 SD490	D22 SD490	2-D10	300 (0.75Dj)	100	75 (3d)
	No.2	70									
	No.3	36									
	No.4	21	J								
	No.5	21						4-D10			
B	No.7	50	J			D25 USD 685	D22 SD490	2-D10	300 (0.75Dj)	100	75 (3d)
	No.8	70	B								
	No.9	36	J								
	No.10	50									
	No.11	50	B	400 x 400	530 x 600	D32 USD 685	D25 SD490		384 (0.64Dj)	216	100 (3.1d)
	No.12	50	J	400 x 400	350 x 450		D25 SD490		300 (0.75Dj)	100	85 (2.7d)

B=Beam yielding, J=Beam Column Joint shear failure, B→J: beam yielding prior to joint shear failure
Dj: Column Depth, d: main bar diameter, joint lateral reinforcement pitch=100 mm, Fc:N/mm^2

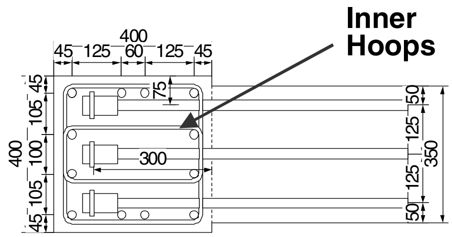

Fig. 3 Joint section

The horizontal development length of mechanical anchorage is 0.75 times the depth of column (300 mm) and 12 times the diameter of beam main bars (D25, diameter of 25 mm). The rear covering depth is 100 mm and the side covering depth is 75 mm (measured from the center of the bars), which represents three times a D25 bar diameter, as shown in Fig. 3.

The mechanical anchorage device, shown in Fig. 4, is a cast iron that is fixed at the end of screw type hot rolled bar. The bearing area of anchor plate is about 6.5 times the bar section as shown in Fig. 5. The specimens were manufactured in horizontal position, therefore it generates from the concrete casting direction, lower, middle and upper bars, which will be analyzed separately in the last sections of this paper.

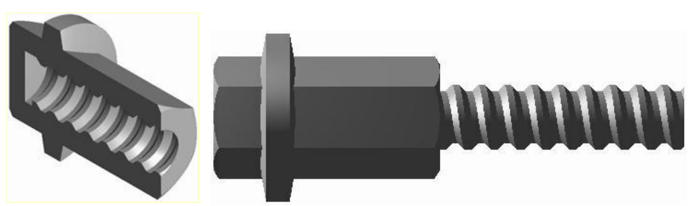

Fig. 4 Mechanical device

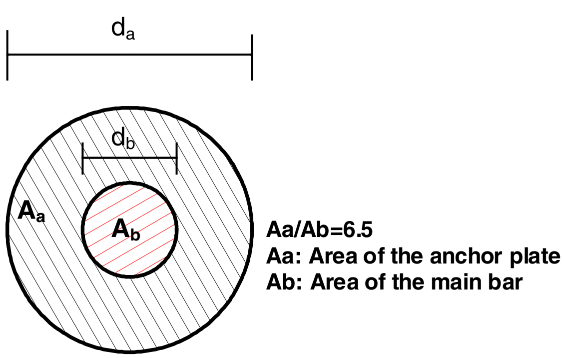

Fig. 5 Anchor plate bearing area

Loading System and Instrumentation

The specimens were subjected to simulated cyclic loads by mean of vertical forces applied through the actuator at the beam end as shown in Fig. 6. The axial force applied on the top of the column was maintained constant during the experiments. The loading history was controlled in terms of lateral drift angle as follow: once at R=1/800, then twice at 1/400, 1/200, 1/100, 1/50, 1/25, as shown in Fig. 7. The lateral drift angle (R=δ/L) is defined as the displacement of the beam (δ) divided by length (L) between the loading point and the center of the column.

Transducers recorded the total and partial deformations of the specimens as shown in Fig. 8. Also strain gauges were placed in the groove cut (4mm wide and 3mm deep) along rib of beam main bar as shown in Fig. 9.

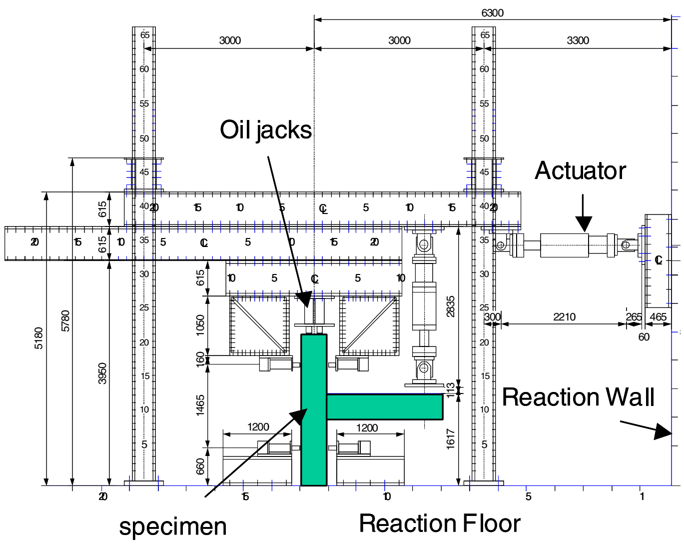

Fig. 6 Loading system

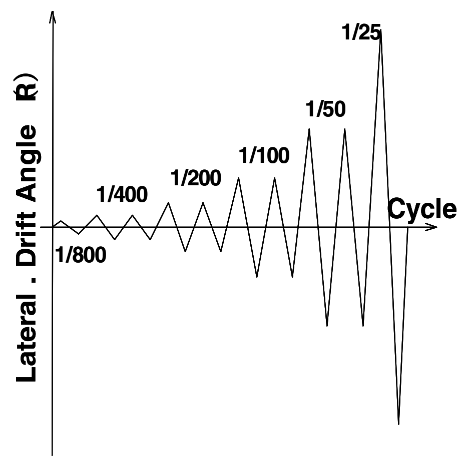

Fig. 7 Loading history

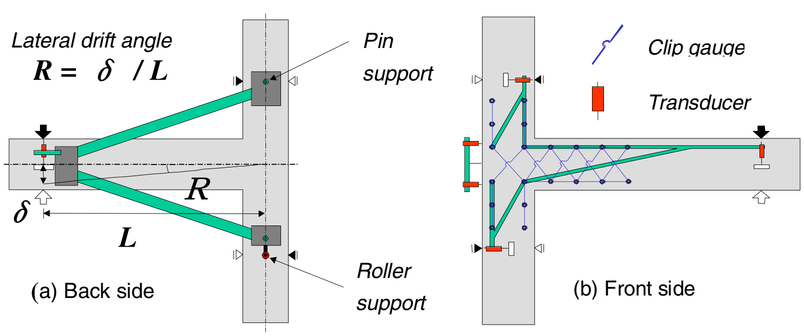

Fig. 8 Instrumentation

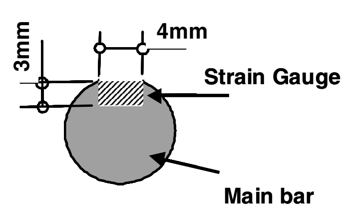

Fig. 9 Location strain gauge

Materials Properties

The mechanical properties of the concrete and steel bars are shown in Tables 2 and 3.

Table 2 Concrete properties

Fc	Compressive strength (N/mm^2)			E	σ_t
	Moist curing 28 d	Dry curing			
		28 d	Exp. day		
21	23.6	20.3	26.9	24.2	2.19
36	37.7	35.2	44.3	28.2	3.16
50	57.7	44.9	49.0	28.5	3.17
70	62.4	51.2	61.1	29.0	3.70

Fc: Specified concrete strength (N/mm^2)
E: Young's modulus (kN/mm^2), d: days
σ_t: Tensile Strength (N/mm^2)

Table 3 Steel properties

Size	Grade	σ_y	σ_t	E	μ_y
D10	SD295A	369	495	184	2010
	USD685	812	948	205	4050
D13	USD685	743	921	205	3670
D22	SD490	571	757	204	2980
D25	SD390	444	638	200	2540
	SD490	560	767	201	3090
	USD685	605	870	199	3040
D32	USD685	595	845	205	2902

σ_y: Yielding Strength (N/mm^2), μ_y: Yielding Strain
σ_t: Tensile Strength (N/mm^2)
E: Young's Modulus (kN/mm^2)

TEST RESULTS

Crack Pattern

Crack patterns at the final loading cycle (R=1/25) for typical specimens are shown in Fig. 10.

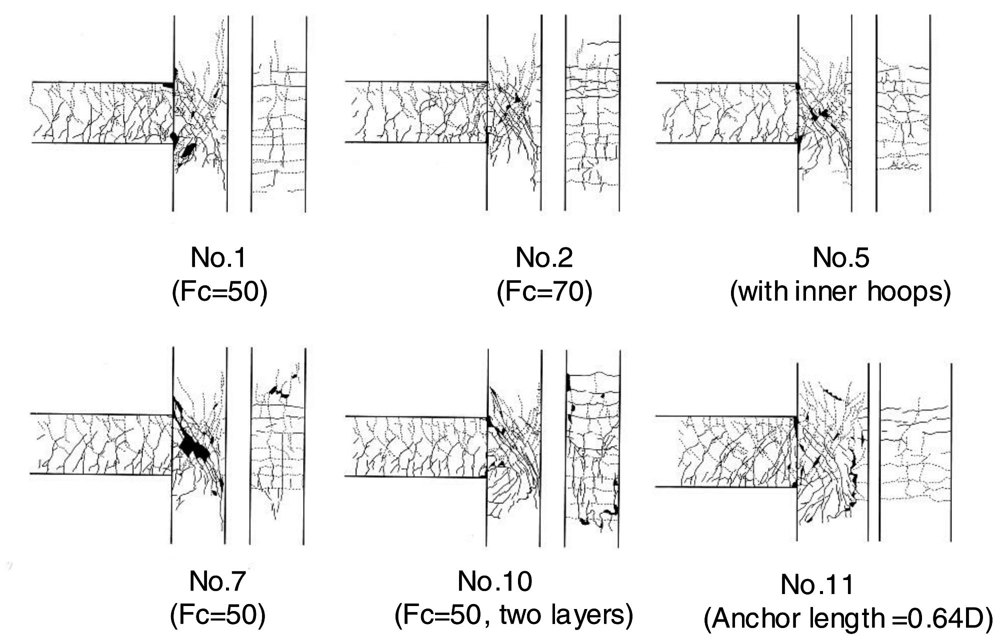

Fig. 10 Crack patterns

Series A
Specimens No.1 to No.3 with beam bending type failure (J), presented fewer shear cracks at the joint panel and cracks at the rear side of the column as much as the concrete strength was increased.

Specimens No.4 and No.5 with joint shear type failure (J), the diagonal cracks started to form on the joint at R=1/400 and continued to growing remarkable as the lateral displacement was increased, leading to the spalling of cover concrete at R=1/25. For Specimen No.4 vertical cracks occurred along main bars at the rear side of column, probably because the beam main bars were pushed out at the compression side. On the other hand, Specimen No.5 with inner hoops presented fewer cracks at the rear side of the column.

Series B
For Specimen No.10 the shear cracks appeared at R=1/400 and for Specimen No.12 in the next loading stage at R=1/200. Both specimens showed widely opened shear cracks, and comparing with other specimens of this series the joints were severely damaged at the rear side of the column, with the concrete spalling off due to compression failure.

Among Specimens No.7, No.8, No.9 and No.11 the lower concrete strength was used, the more shear cracks were observed at the joints. Especially Specimen No.9 presented severe damage on the rear side of the columns. On the other hand, Specimen No.11 with larger beam and column sections presented fewer shear cracks at the joints and the rear side of the column.

Load Displacement
Beam load-displacement relationships are presented in Fig. 11. For all specimens, the beam yielded in flexure at R = 1/100, and maximum strength was reached at R = 1/50. In the case of specimens with joint shear failure (J failure), after the positive cycle of R=1/25 the hysteresis loops showed pinching effect as a consequence of the severe cracking on the joints.

Series A
Specimen No.2 developed B type failure, while Specimens No.1 and No.3 were judged as shear failure type at beam column joint after beam flexural yielding (B→J). Among these specimens, as concrete strength was decreased, the ultimate shear strength become lower, with a tendency to have considerable strength decay after the peak of strength.

Specimens No.4 and No.5 failed in shear at the joints (J). Specimen No.4 showed significant strength decay after reaching the peak of strength, because of the loose of anchorage of the main bars due to joint shear failure. However, Specimen No.5 showed a more stable hysteresis loops with moderate strength decay, which is consequence of the inner hoops placed at the joint.

Series B
Specimens No.7 to No.9 and No.11 failed in shear at joint after beam flexural yielding (B→J). On the other hand, Specimens No.10 and No.12 had shear failure at the joint (J). Specimens No.7 to No.9 with similar hysteresis loops showed no influence of the different concrete strength. In case of Specimen No.11 with anchor length of 12d (d: bar diameter), which represent the 0.64Dj, the maximum strength did not reach the ultimate joint shear strength. After the peak strength the loops showed considerable strength decay. On the other hand, the Specimen No.12 which has an anchor length shorter than 12d which represents a development length of 0.75Dj, showed adequate ultimate joint shear strength.

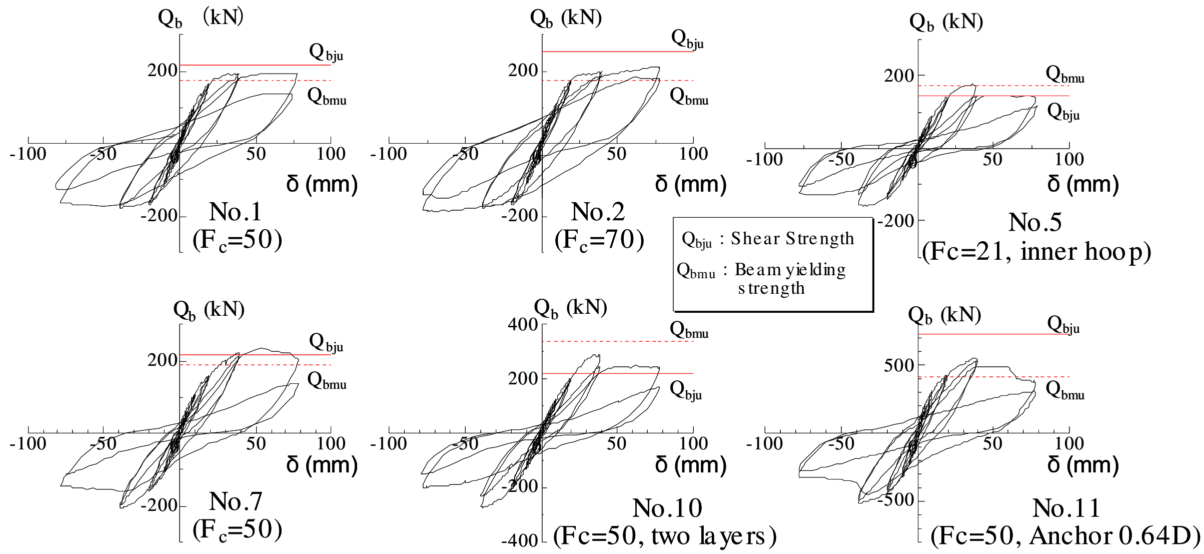

Fig. 11 Beam load-displacement relationship

Deformation Capacity

Table 4 shows the deformation capacity of specimens, at 80% (R80) and 95% (R95) of the maximum strength, respectively. The obtained deformation capacity, about 0.02 to 0.03 rad. for R95, and 0.04 rad. for R80, showed no differences among all specimens. However, Specimen No.11, with an anchorage length of 0.64Dj, showed R80 at a lateral drift angle of 0.032 rad., which indicates they have poor deformation capacity compared with other specimens.

In the case of J failure type specimens, the joint deformation always increases with loading stages, leading to the final shear failure. For Specimen No. 5 the joint deformation capacity rate showed very small value, indicating the inner hoops placed inside the joint panel worked effectively.

Table 4 Deformation capacity

Spec.	Parameter	F_c	σ_B	Failure Mode	Lateral Drift Angle	
		N/mm^2			R95	R80
No.1	A Series - Basic	50	49	B→J	0.04	0.040
No.2	F_c - High	70	61	B	0.04	0.040
No.3	F_c – Low-1	36	44	B→J	0.022	0.040
No.4	F_c – Low-2	21	27	J	0.020	0.040
No.5	Inner hoop	21	27	J	0.020	0.039
No.7	B Series - Basic	50	49	B→J	0.035	0.040
No.8	F_c - High	70	61	B→J	0.033	0.041
No.9	F_c – Low	36	44	B→J	0.025	0.041
No.10	Double layer reinf.	50	49	J	0.026	0.039
No.11	Anchor length (long)	50	49	B→J	0.024	0.032
No.12	Anchor length (short)	50	49	J	0.023	0.040

Deformation Components

The deformation rate of each member (beam, column, joint) to the total deformation is shown if Fig. 12, for some representative specimens. The curvature and the shear strain measured every 20 cm for each member was used to calculate the deformation rate.

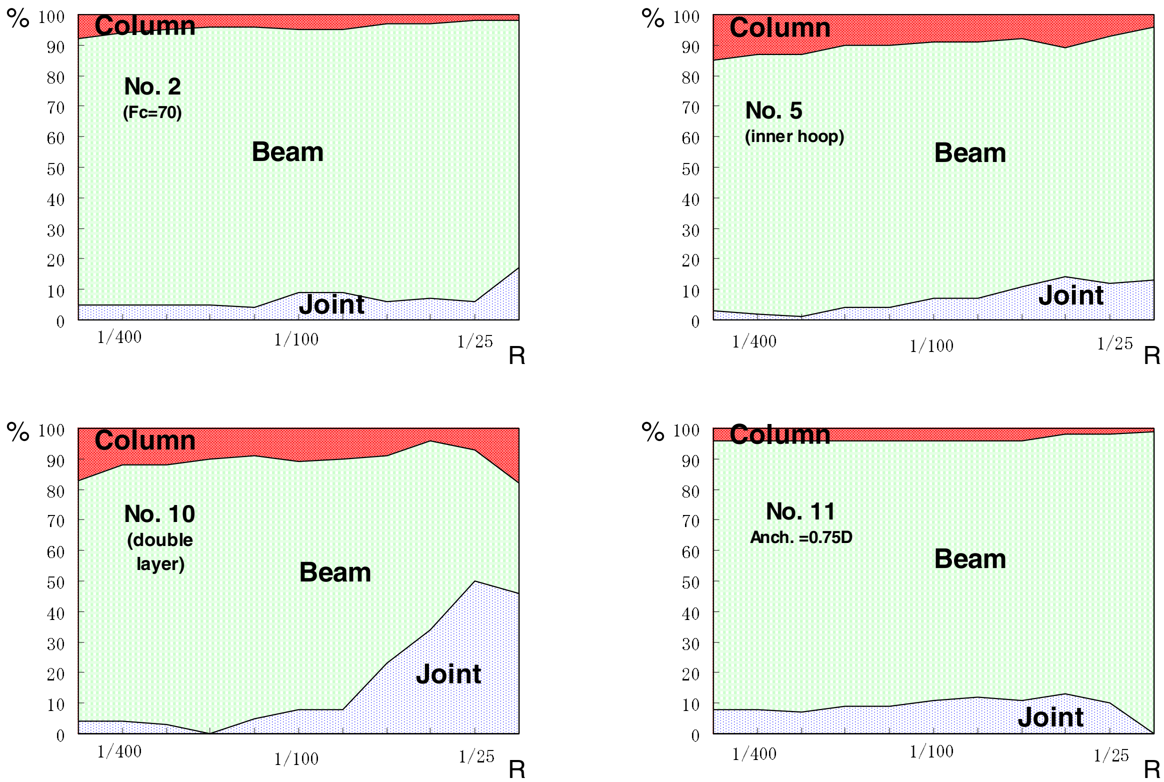

Fig. 12 Deformation components

The beam made the bigger contribution to the total deformation in the case of specimens with B failure type and B→J failure type. After the beam reach the yielding at R=1/50, the beam deformation increased for a while, but in the further loading stages the reverse phenomenon was observed.

In the case of J failure type specimens the joint deformation always increases with loading stages, leading to the final shear failure. The deformation components showed good correspondence with the final failure patterns of the specimens.

In the case of Specimen No.5, the joint deformation rate showed a very small value, indicating the inner hoops placed inside the joint panel worked effectively. On the other hand, in the case of Specimen No.10 with beam reinforcement placed in 2 layers, the joint deformation was particularly bigger compared with other specimens.

Maximum Strength

The comparison between the experimental values Q_{bu} expressed in terms of beam shear force, and the calculated values like bending strength Q_{bmu}, the joint shear strength Q_{bsu}, and the anchorage strengths of beam main bars Q_{ba}, all calculated as beam load are shown in Fig. 13.

In the case of specimens where the experimental value Q_{bu} was smaller than Q_{bmu}, they showed joint shear failure and the experimental values were close to the calculated ones. For specimens where the experimental value Q_{bu} was higher than Q_{bmu} showed good correspondence with the final failure patterns. Specimen No.5 showed a little higher strength, compared with No.4, due to the effect of inner hoops placed in the joint.

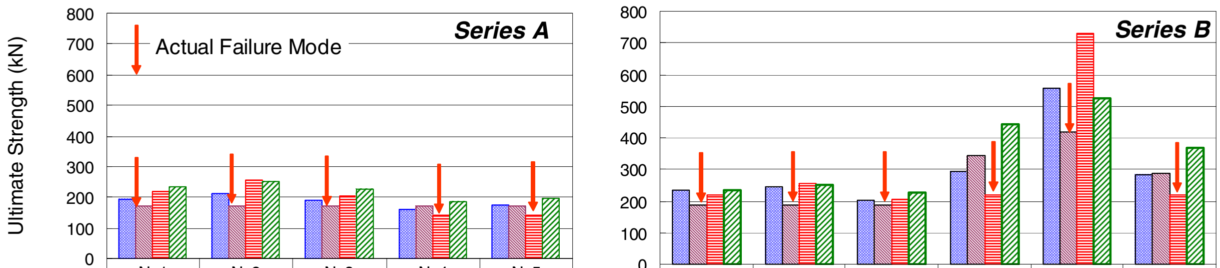

	No1	No2	No3	No4	No5
Qbu	195	212	190	161	177
Qbmu	173	173	173	173	173
Qbsu	219	256	204	144	144
Qba	235	251	227	187	196

	No7	No8	No9	No10	No11	No12
Qbu	235	245	201	293	554	282
Qbmu	187	187	187	343	417	288
Qbsu	219	256	204	219	730	219
Qba	235	251	227	442	524	367

Fig. 13 Ultimate shear strength (Units: kN)

a) Ultimate shear strength of beam-column-joint (Q_{ju})

$Q_{ju} = k \cdot \phi \cdot F_j \cdot b_j \cdot D_j$, *given by* AIJ [4]

Here:

$F_j = 1.6\,\sigma_B^{\ 0.7}$, $k = 0.7$, $\phi = 0.85$, b_j =*effective joint width,* D_j =*column depth*

b) Anchorage Strength (σ)

$\sigma = k \cdot \sigma_{std}$ where $\sigma_{std} = 324\sqrt{\sigma_B}$ and $k = k_1 \cdot k_2 \cdot k_3$) given by Murakami [1], [2].

σ_B= concrete strength (Units: σ and σ_B are in kgf/cm^2)

k_1 =1, Coefficient depending on the ratio of the bearing area of mechanical anchorage to bar section

k_2 =0.96+0.01 (C/d_b), coefficient representing the influence of the cover depths

(C= cover depth, d_b=nominal bar diameter)

k_3 = Coefficient representing the influence of the lateral reinforcement (only the outer hoops are considered)

$$k_3 = 62.5 \cdot p_{wj} - 0.12 p_{wj} \cdot (\sigma_B - 277) + 1 \quad \text{(in case } p_{wj} \leqq 0.4\% \text{)}$$

$$k_3 = 12.5 - 0.05 \cdot (\sigma_B - 277) \quad \text{(in case } p_{wj} > 0.4\% \text{)}$$

p_{wj} = lateral reinforcement ratio in the beam-column-joint

Shear stress-shear deformation relationship

The joint shear stress-shear deformation relationship is shown in Fig. 14. The average joint shear stress is calculated using the effective joint shear area b_j x D_j, where bj is the effective width of the beam column joint panel (average of the beam and column width) and D_j is the anchorage length of the main bars into the joint panel. The joint shear trains (γ) were obtained from the diagonal clip gauges attached to the joint as shown in Fig. 8.

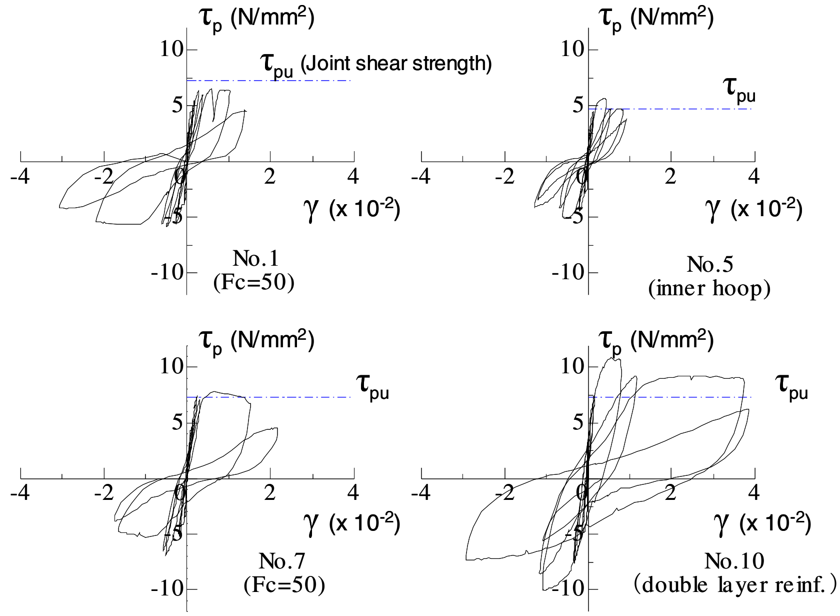

Fig. 14 Shear stress-shear deformation relationship

For specimens with B and B→J failure type, at the beam yielding stage, the shear deformation tend to increase as much as the concrete strength decrease, independently on the differences of the main bars. After the yielding at R=1/25, shear failure was observed.

For the J failure type specimens (No.4, No.5, No.10, No.12), at R=1/50, the shear stress surpass the calculated joint shear strength (τ_{pu}) reaching the joint failure. In case of specimen No.5, showed very small amount of joint shear strains, and were half of those obtained for specimen No.4, showing the effect of the inner hoops placed in the joint reinforcement. Specimen No.10 with beam bars placed in double layer, failed in joint shear with larger shear deformation.

Strain Distribution of main bars

Typical strain distributions of beam main bars are shown in Fig. 15. The figures show the strain distribution of the bar that was located in the upper side when the specimens were cast, as shown in Fig. 16. The specimens with B or B→J failure type, at a lateral drift angle R=1/100 strains of main bars start to reach the yield point at the column face. At R=1/50, in the vicinity of the anchor plate (inside of the joint), the strains did not reached the yielding, then it is possible to infer that at this loading stage the main bars were still bearing the external forces by bond stresses.

In the case of Specimen No.5 with J failure type, the strains of main bars developed steadily with the loading increase, and did not reach the yielding limit even at R=1/25. Comparing with the B type failure specimens, the strains showed the tendency to become bigger near the anchor plate. This is because the concrete at the joint panel became heavily damaged since the early stages of loading, causing the loose of the adherence of the main bars inside of the joint. At this stage, the anchor plate mainly sustained the external forces. This shows that the progress of the strains of main bars is closely related with the failure pattern.

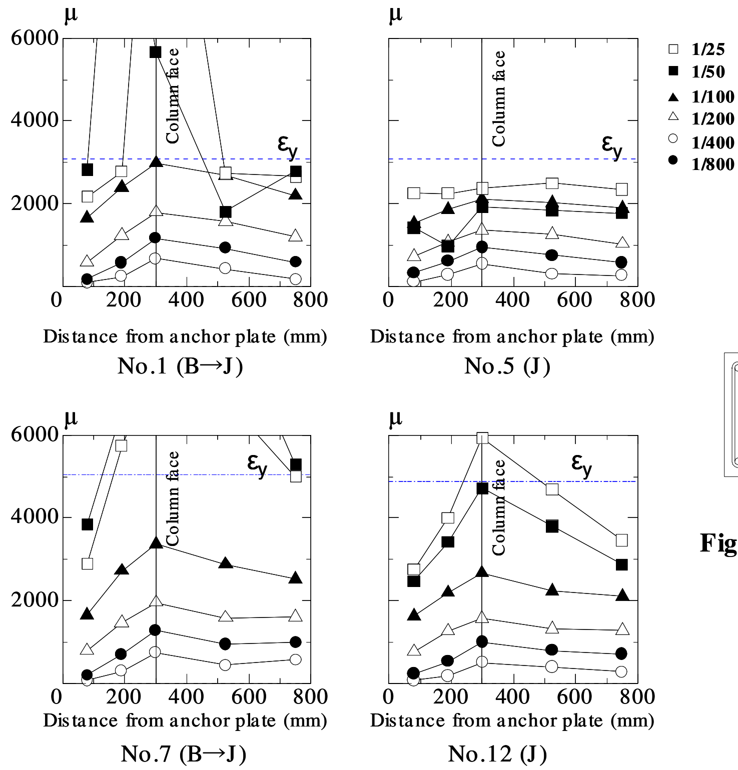

Fig.15 Strain distribution

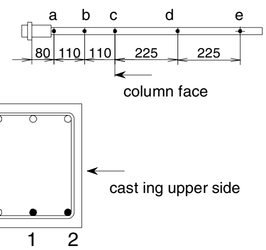

Fig.16 Location of strain gauges

Contribution to Bearing Force by the Anchor Plate

The tension forces developed in the beam bars are to be resisted inside the joint, by a combination of bond stresses of main bars and bearing stresses in the anchor plate. The contribution to resist the tension forces, given by each of these mechanisms is shown in Fig. 17.The strains recorded by stain gauges at the positions "*a*", shown in Fig. 16, were used to calculate the resistance force provided by the anchor plate. The strains recorded in the position "*c*" were used to calculate the tension force acting on the main bars.

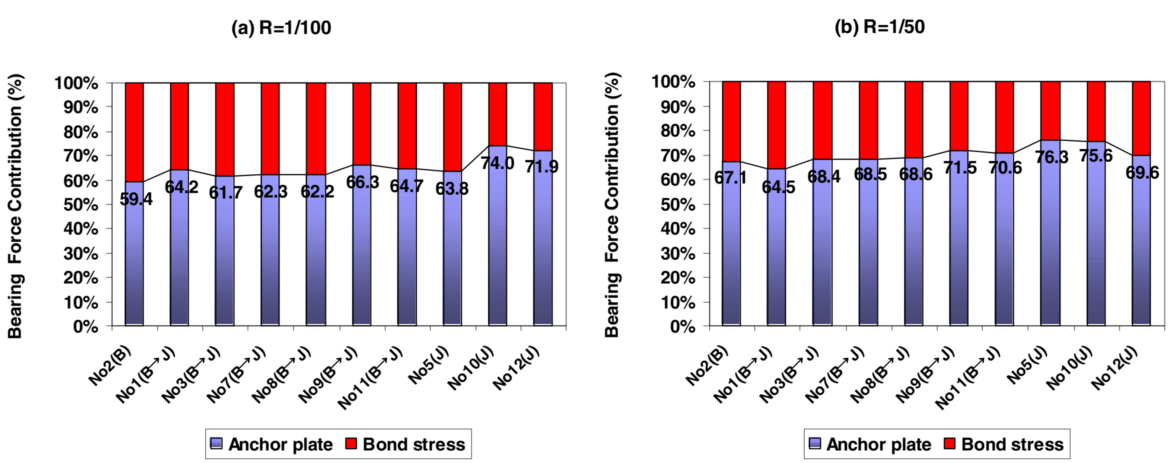

Fig. 17 Contribution to the bearing force

In case of specimens with B and B→J failure type, at R=1/100 the anchor plate carried about the 60% of the bearing force. When the lateral drift angle becomes R=1/50 the anchor plate carrying force increased to 70%. On the other hand, in case of J failure type at R=0.01 the anchor plate carrying force fluctuates between 65 to 75%. At this stage the main bars might have loose adherence because of the shear failure of the joint, therefore the anchor plate carries most of the bearing force.

Relation between the anchor plate stress and its displacement

The relations between the applied load and the displacement of the anchor plate, is shown in Figs. 18 and 19. For the calculation of the average bearing stresses acting on the anchor plate, the strains of the main bars near the anchor plate and the section of the device perpendicular to their axis were used. The displacement, which was recorded from the rear part of the column, represents the pull out of the anchor plate. This displacement value includes the cracks width.

The plate displacement ranged between 1 to 2 mm when the load peak was reached, growing rapidly after this point. Larger displacements were observed for the upper bars. Same tendency was observed for all specimens.

In case of specimens with B and B→J failure the displacements was negligible, about 1 mm, before the flexural yielding. After the yielding the displacement increased considerably becoming within 7 mm and 16 mm at the final stage for the upper bars. On the other hand for the middle bars the displacement was less than 10 mm.

In case of specimens with joint shear, the anchor plate displacement increased rapidly by R=1/50, approximately 3 mm. At this stage the shear failure happened at the joints. For Specimen No.5 (inner hoops) even after the shear failure, the displacement of the anchor plate was restrained to a very small value, comparing with other specimens. This shows the effect of the inner hoops.

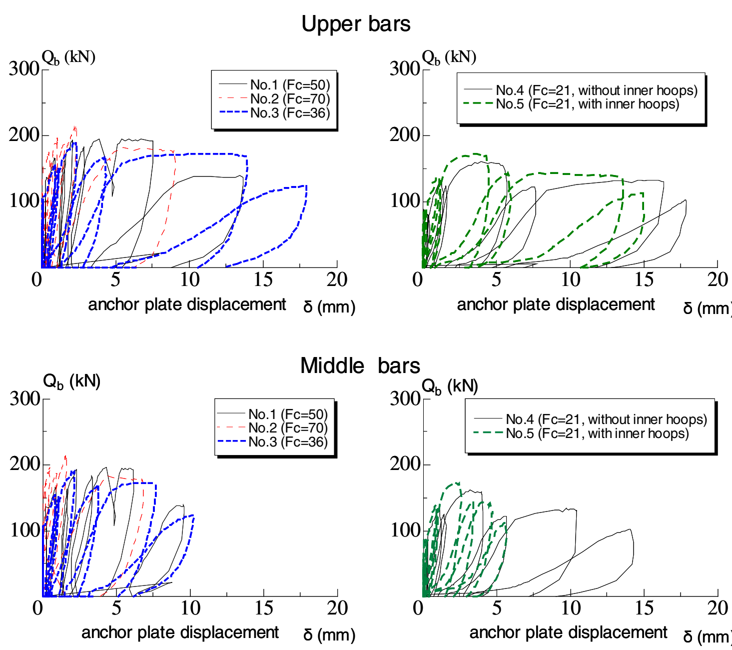

Fig. 18 Anchor plate displacement for SD490 bars

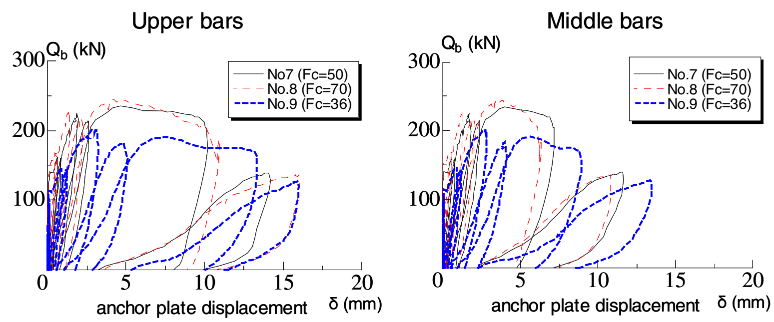

Fig. 19 Anchor plate displacement for SD685 bars

CONCLUSIONS

The following conclusions can be drawn from the test results:

1) The crack patterns showed good correspondence with the design failure, especially for the specimens joint shear failure. In addition, the cracks on the rear side of the column were well controlled by adding the inner hoops.
2) The inner hoops played an important role not only in the control the strength decay after the maximum strength was reached, but also avoiding an excessive displacement of the anchor plate.
3) For the specimen with lower concrete strength (Fc=24 N/mm^2), since the bond deterioration starts in the early stages the anchor plate resistant contribution became also important in these stages.
4) For exterior beam column joints with mechanical anchorage, provided that concrete cover of main bar (measured from the center of the bar) is 3 times the bar diameter, anchor length is 3/4 times the column depth and 12 times the bar diameter, enough anchor strength can be attained.
5) For specimens with bending failure type, before the beam reached the yielding, the anchor plate displacement was very small. However, for specimens that failed in joint shear after the beam yielding showed bigger displacements at the final loading stages.
6) For specimens with joint shear failure, the joint shear distortion influenced the anchor plate displacement.

REFERENCES

1. Masahide Murakami et. al.: Development on High Strength Reinforcement of Electric Furnace Part 21, Estimation on Mechanical Anchorage Capacity (in Japanese), Summaries of Technical Papers of Annual Meeting, Architectural Institute of Japan, C- Structures II, pp. 127-128, 1993.
2. Toshiyuki Kubota and Masahide Murakami: Failure Behavior of External Beam Column Joints with Mechanical Anchorages (in Japanese), Proceedings of the Japan Concrete Institute Vol.17, No.2, pp. 1189-1194, 1995.
3. Imai H., Shibata K.: Experimental Study on The Structural Performance of Mechanical Anchorage in Beam Column Joints of RC Exterior Subassemblage, Proceedings of 6th International Conference on Appraisal, Repairs and Maintenance of Buildings and Structures, Melbourne, Dec. 1999, pp. 173-180.
4. Architectural Institute of Japan: Design Guidelines for Earthquake Resistant Reinforced Concrete Buildings Based on Inelastic Displacement Concept, (in Japanese), 1997.